

# Monitoring statistics of the ERS-2 scatterometer for ESA

## Cycle 123

(Project Ref. 18212/04/I-OL)

Hans Hersbach

European Centre for Medium-Range Weather Forecasts,

Shinfield Park, Reading, RG2 9AX, England

Tel: (+44 118) 9499476, e-mail: dal@ecmwf.int

February 28, 2007

## 1 Introduction

The quality of the UWI product was monitored at ECMWF for Cycle 123. Results were compared to those obtained from the previous Cycle, as well for data received during the nominal period in 2000 (up to Cycle 59). No corrections for duplicate observations were applied.

During Cycle 123 data was received between 21:04 UTC 22 January 2007 and 20:58 UTC 26 February 2007. Received data was grouped into 6-hourly batches (centred around 00, 06, 12 and 18 UTC). No data was received for such batches between 18 UTC 23 January and 18 UTC 24 January 2007 (due to a one-day delay in the UWI dissemination chain), 06 UTC 25 January 2007 and 00 UTC 7 February 2007. Data is being recorded whenever within the visibility range of a ground station. Data coverage for Cycle 123 was over the North-Atlantic, the Mediterranean, the Caribbean, the Gulf of Mexico, a small part of the Pacific west from the US, Canada and Central America, the Chinese and Japanese Sea, a small part of the Indian Ocean South-East of Thailand and Indonesia, and the Southern Ocean around Australia and New Zealand (see Figure 2).

The asymmetry between the fore and aft incidence angles showed a few isolated peaks. The data was flagged accordingly by the combined yaw- $k_p$  flag. The Sun is still near a period of minimal activity. The Earth was under influence of a solar wind stream around 14 February 2007 (source: [www.spaceweather.com](http://www.spaceweather.com)). There was no sign that this event had affected ERS-2 attitude control.

Compared to Cycle 122, the UWI wind speed relative to ECMWF first-guess (FG) fields showed a somewhat higher standard deviation (1.60 m/s, was 1.55 m/s).

Bias levels were slightly less negative (-0.86 m/s, was -0.77 m/s).

Ocean calibration shows that inter-node and inter-beam dependencies of bias levels are similar to those during Cycle 122. Average bias levels were stable (-0.41 dB, unchanged; see Figure 4).

The ECMWF assimilation/forecast system was not changed during Cycle 123.

The Cycle-averaged evolution of performance relative to ECMWF first-guess (FG) winds is displayed in Figure 1. Figure 2 shows global maps of the over Cycle 123 averaged UWI data coverage and wind climate, Figure 3 for performance relative to FG winds.

## **2 ERS-2 statistics from 23 January to 26 February 2007**

### **2.1 Sigma0 bias levels**

The average sigma0 bias levels (compared to simulated sigma0's based on ECMWF model FG winds) stratified with respect to antenna beam, ascending or descending track and as function of incidence angle (i.e. across-node number) is displayed in Figure 4.

Inter-node and inter-beam dependencies are similar to Cycle 122, as well as average levels (-0.41 dB, unchanged), being around 0.05 dB less negative than for nominal data in 2000 (see Figure 1 of the reports for Cycle 48 to 59). The situation is similar to that of one year ago (see Cyclic report 113). Long-term variations correlate with the yearly cycle, which, given the non-global coverage, is understandable. Therefore, the method of ocean calibration will probably only provide accurate information on calibration levels for globally or yearly averaged data sets.

The data volume of descending tracks was lower (by 21%) than for ascending tracks.

### **2.2 Incidence angles**

For ESACA, across-node binning is, like the old processor, retained on a 25km mesh. From simple geometrical arguments it follows that variations in yaw attitude will lead to asymmetries between the incidence angles of the fore and aft beam. Indeed, this has been observed. Figure 5 gives a time evolution of this asymmetry. Also in this Figure, the occasions for which the combined  $k_p$ -yaw quality flag was set are indicated by red stars. The relation with incidence-angle asymmetries is obvious.

Several isolated peaks emerged, the largest occurring on 26 January, 4 February, 16 February and 20 February 2007. The data was flagged accordingly by the combined yaw- $k_p$  flag. The Sun is near a period of minimal activity. Although, a solar wind stream did hit the Earth around 14 February 2007 (source: [www.spaceweather.com](http://www.spaceweather.com)). These events did not coincide with peaks in the ERS-2 attitude time-series.

## 2.3 Distance to cone history

The distance to the cone history is shown in Figure 6. Curves are based on data that passed all QC, including the test on the  $k_p$ -yaw flag, and subject to the land and sea-ice check at ECMWF (see cyclic report 88 for details).

Like for Cycle 122, time series are (due to lack of statistics) very noisy, especially for the near-range nodes. Most spikes were found to be the result of low data volumes.

Compared to Cycle 122, the average level was slightly higher (1.17), which is about 7% higher than for nominal data (see top panel Figure 1).

The fraction of data that did not pass QC is displayed in Figure 6 as well (dash curves). Peaks often coincides with peaks in yaw anomaly.

## 2.4 UWI minus First-Guess wind history

In Figure 7, the UWI minus ECMWF first-guess wind-speed history is plotted.

The history plot shows a few peaks, which are usually the result of low data volume.

Figure 11 displays the locations for which UWI winds were more than 8 m/s weaker (top panel) and more than 8 m/s stronger (lower panel) than FG winds. Like for Cycle 122, such collocations are isolated, and often indicate meteorologically active regions, for which UWI data and ECMWF model field show reasonably small differences in phase and/or intensity. Deviations near the poles are the result of imperfect sea-ice flagging.

Two cases where UWI and ECMWF wind speed differ significantly are presented in Figure 12. Top panel shows a complex situation of two merging low pressure systems south of Greenland for 6 February 2007. For the right-hand system the scatterometer winds show a less elongated and slightly shifted vortex. Although the UWI winds look sensible, they do suffer from incorrect de-aliasing near the centre.

The lower panel shows a case in the North Atlantic for 10 February 2007. In general ECMWF and UWI compare well. However, near the centre of the low, the under-estimation of UWI winds is mainly due to the saturation of the CMOD4 model function for strong winds (better for CMOD5, not shown).

Average bias levels and standard deviations of UWI winds relative to FG winds are displayed in Table 1. From this it follows that the bias of both the UWI and CMOD4 product has become somewhat less negative (from -0.86 m/s to -0.78 m/s), being around 0.1 m/s less negative to the level of nominal data in 2000.

On a longer time scale seasonal bias trends are observed (see Figure 1). As was highlighted in previous cyclic reports, it is believed that this yearly trend is partly induced by changing local geophysical conditions. Strong indication for this is a similar trend observed for QuikSCAT data when restricted to an area well-covered by ERS-2 (20N-90N, 80W-20E). Figure 17 shows time series for that area for both ERS-2 (top panel) and QuikSCAT (lower panel) for the period between 1 January 2004 and 26 February 2007 (end of Cycle 123). Results are displayed for at ECMWF actively assimilated data, i.e., CMOD5 winds for ERS-2 and 4%-reduced QuikSCAT

	Cycle 122		Cycle 123	
	UWI	CMOD4	UWI	CMOD4
speed STDV	1.55	1.54	1.60	1.59
node 1-2	1.65	1.61	1.63	1.60
node 3-4	1.54	1.52	1.55	1.53
node 5-7	1.49	1.48	1.53	1.52
node 8-10	1.48	1.47	1.56	1.56
node 11-14	1.50	1.50	1.58	1.59
node 15-19	1.52	1.53	1.57	1.58
speed BIAS	-0.86	-0.85	-0.78	-0.77
node 1-2	-1.49	-1.45	-1.39	-1.36
node 3-4	-1.18	-1.12	-1.12	-1.07
node 5-7	-0.90	-0.87	-0.84	-0.81
node 8-10	-0.70	-0.70	-0.62	-0.61
node 11-14	-0.65	-0.66	-0.55	-0.56
node 15-19	-0.64	-0.66	-0.55	-0.57
direction STDV	28.4	18.8	30.8	19.8
direction BIAS	-2.5	-2.3	-1.7	-1.5

Table 1: Biases and standard deviation of ERS-2 versus ECMWF FG winds in m/s for speed and degrees for direction.

winds on a 50km resolution.

The standard deviation of UWI wind speed versus ECMWF FG was, compared to Cycle 122, slightly enhanced (1.56 m/s, was 1.60 m/s).

For Cycle 123 the (UWI - FG) direction standard deviations were mostly ranging between 20 and 40 degrees (Figure 8), representing nominal variations. Averaged over the entire cyclic period, STDV for UWI wind direction has slightly grown (30.8 degrees, was 28.4 degrees). For at ECMWF de-aliased winds a similar trend was observed (STDV 19.8 degrees, was 18.8 degrees).

## 2.5 Scatterplots

Scatterplots of FG winds versus ERS-2 winds are displayed in Figures 13 to 16. Values of standard deviations and biases are slightly different from those displayed in Table 1. Reason for this is that, for plotting purposes, the in 0.5 m/s resolution ERS-2 winds have been slightly perturbed (increases scatter with 0.02 m/s), and that zero wind-speed ERS-2 winds have been excluded (decreases scatter by about 0.05 m/s).

The scatterplot of UWI wind speed versus FG (Figure 13) is very similar to that for (at ECMWF inverted) de-aliased CMOD4 winds (Figure 15). It confirms that the ESACA inversion scheme is working properly.

Winds derived on the basis of CMOD5 are displayed in Figure 16. The relative standard deviation is lower than for CMOD4 winds (1.57 m/s versus 1.62 m/s).

Compared to ECMWF FG, CMOD5 winds are 0.23 m/s slower, and there is an enhanced tendency for under-estimation at strong winds.

## Figure Captions

**Figure 1:** Evolution of the performance of the ERS-2 scatterometer averaged over 5-weekly Cycles from 12 December 2001 (Cycle 69) to 26 February 2007 (end Cycle 123) for the UWI product (solid, star) and de-aliased winds based on CMOD4 (dashed, diamond). Results are based on data that passed the UWI QC flags. For Cycle 85 two values are plotted; the first value for a global set, the second one for a regional set (for details see the corresponding cyclic report). Dotted lines represent values for Cycle 59 (5 December 2000 to 17 January 2001), i.e. the last stable Cycle of the nominal period. From top to bottom panel are shown the normalized distance to the cone (CMOD4 only) the standard deviation of the wind speed compared to FG winds, the corresponding bias (for UWI winds the extremes in node-wise averages are shown as well), and the standard deviation of wind direction compared to FG.

**Figure 2:** Average number of observations per 12H and per 125km grid box (top panel) and wind climate (lower panel) for UWI winds that passed the UWI flags QC and a check on the collocated ECMWF land and sea-ice mask.

**Figure 3:** The same as Figure 2, but now for the relative bias (top panel) and standard deviation (lower panel) with ECMWF first-guess winds.

**Figure 4:** Ratio of  $< \sigma_0^{0.625} > / < \text{CMOD4}(\text{FirstGuess})^{0.625} >$  converted in dB for the fore beam (solid line), mid beam (dashed line) and aft beam (dotted line), as a function of incidence angle for descending and ascending tracks. The thin lines indicate the error bars on the estimated mean. First-guess winds are based on the in time closest (+3h, +6h, +9h, or +12h) T511 forecast field, and are bilinearly interpolated in space.

**Figure 5:** Time series of the difference in incidence angle between the fore and aft beam. Red stars indicate the occurrences for which the combined  $k_p$ -yaw flag was set.

**Figure 6:** Mean normalized distance to the cone computed every 6 hours for nodes 1-2, 3-4, 5-7, 8-10, 11-14 and 15-19). The dotted curve shows the number of incoming triplets in logarithmic scale (1 corresponds to 60,000 triplets) and the dashed one indicates the fraction of complete (based on the land and sea-ice mask at ECMWF) sea-located triplets rejected by ESA flags, or by the wind inversion algorithm (0: all data kept, 1: no data kept).

**Figure 7:** Mean (solid line) and standard deviation (dashed line) of the wind speed difference UWI - first guess for the data retained by the quality control.

**Figure 8:** Same as Fig. 7, but for the wind direction difference. Statistics are computed for winds stronger than 4 m/s.

**Figures 9 and 10:** Same as Fig. 7 and 8 respectively, but for the de-aliased CMOD4 data.

**Figure 11:** Locations of data during Cycle 123 for which UWI winds are more

than 8 m/s weaker (top panel) respectively stronger (lower panel) than FG, and on which QC on UWI flags and the ECMWF land/sea-ice mask was applied.

**Figure 12:** Comparison between UWI (red) and ECMWF FG (blue) winds for a case South of Greenland for 6 February 2007 (top panel) and for a case in the North Atlantic for 10 February 2007 (lower panel).

**Figure 13:** Two-dimensional histogram of first guess and UWI wind speeds, for the data kept by the UWI flags, and QC based on the ECMWF land and sea-ice mask. Circles denote the mean values in the y-direction, and squares those in the x-direction.

**Figure 14:** Same as Fig. 13, but for wind direction. Only winds stronger than 4m/s are taken into account.

**Figure 15:** Same as Fig. 13, but for de-aliased CMOD4 winds.

**Figure 16:** Same as Fig. 13, but for de-aliased CMOD5 winds.

**Figure 17:** Wind-speed bias relative to FG winds for actively assimilated ERS-2 winds (based on CMOD5) for nodes 1-19 (top panel) respectively 50-km QuikSCAT (based on the QSCAT-1 model function and reduced by 4%) for nodes 5-34 (lower panel), averaged over the area (20N-90N, 80W-20E), and displayed for the period 1 January 2004 - 26 February 2007. Fat curves represent centred 15-day running means, thin curves values for 6-hourly periods. Vertical dashed blue lines mark ECMWF model changes.

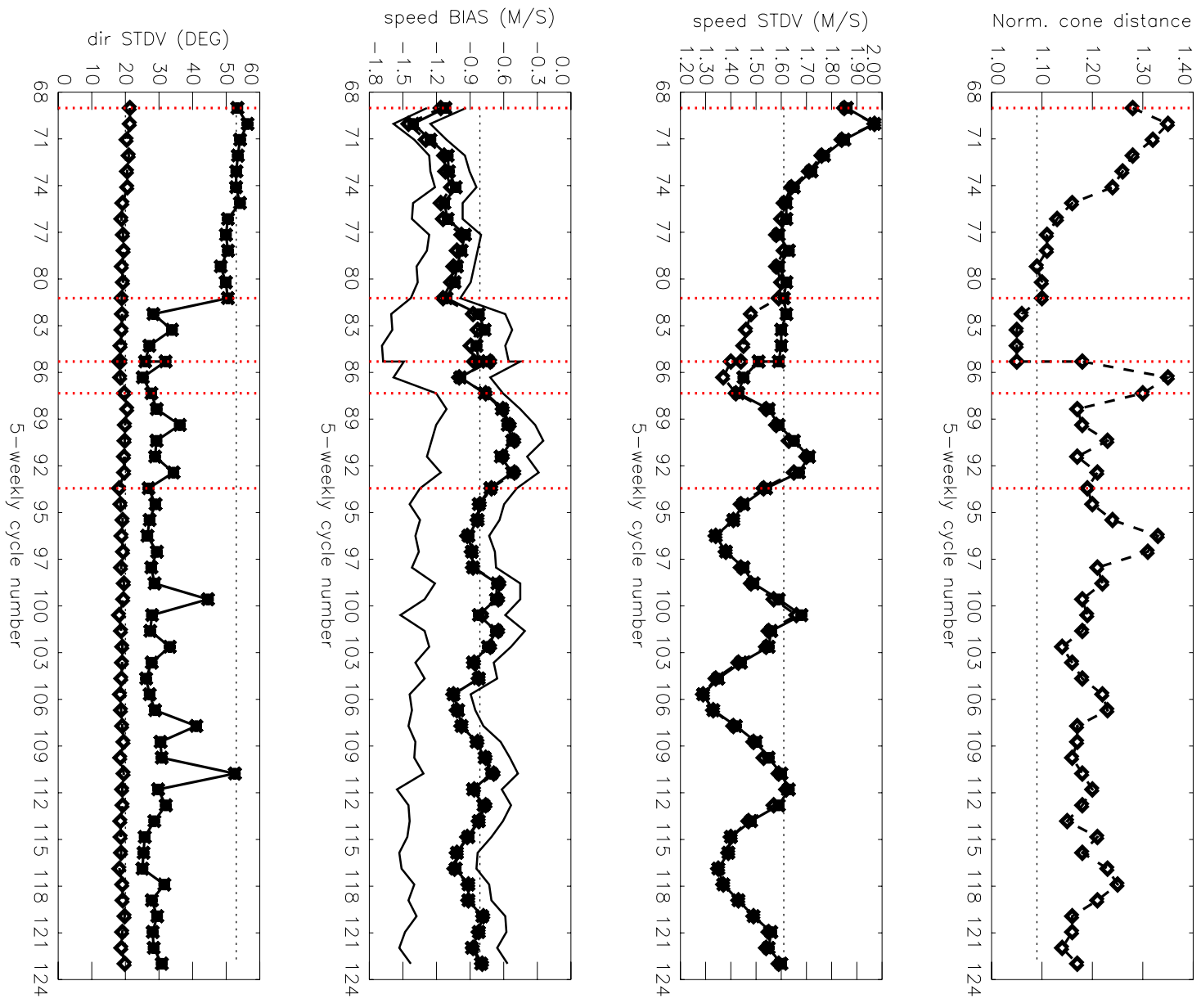
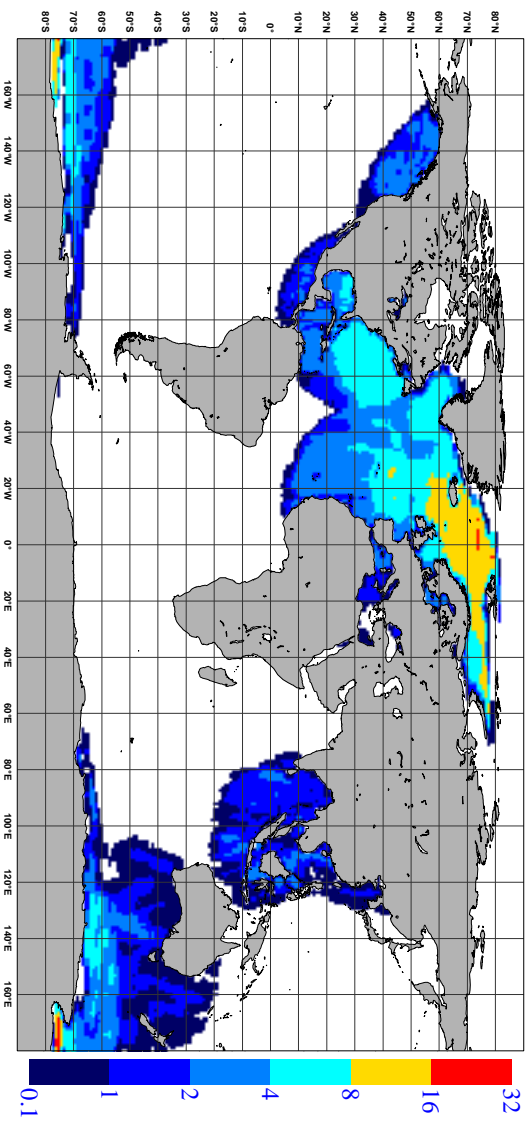


Figure 1

NOBS ( ERS-2 UWI ), per 12H, per 125km box  
average from 2007012300 to 2007022618 GLOB:2.45



AVERAGE ( ERS-2 UWI ), in m/s.  
average from 2007012300 to 2007022618 GLOB:6.78

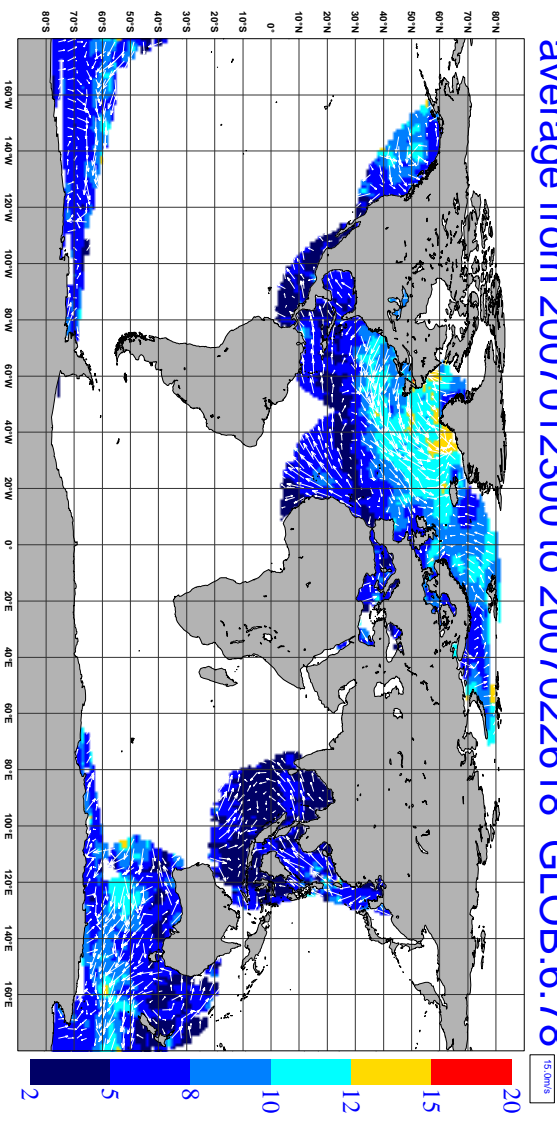
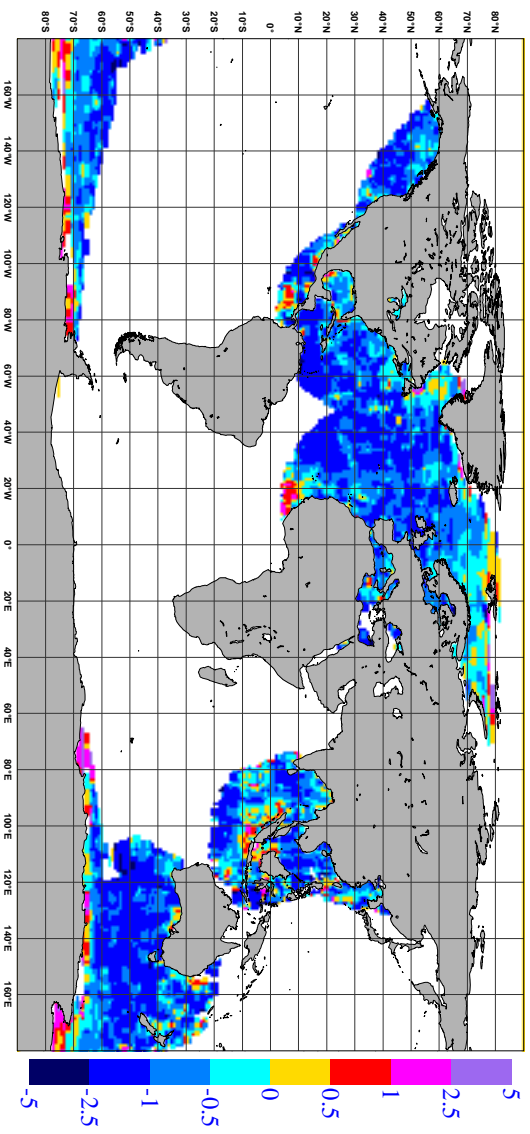


Figure 2



BIAS ( ERS-2 UWI vs FIRST-GUESS ), in m/s.  
average from 2007012300 to 2007022618 GLOB:-0.8



STDV ( ERS-2 UWI vs FIRST-GUESS ), in m/s.  
average from 2007012300 to 2007022618 GLOB:1.2

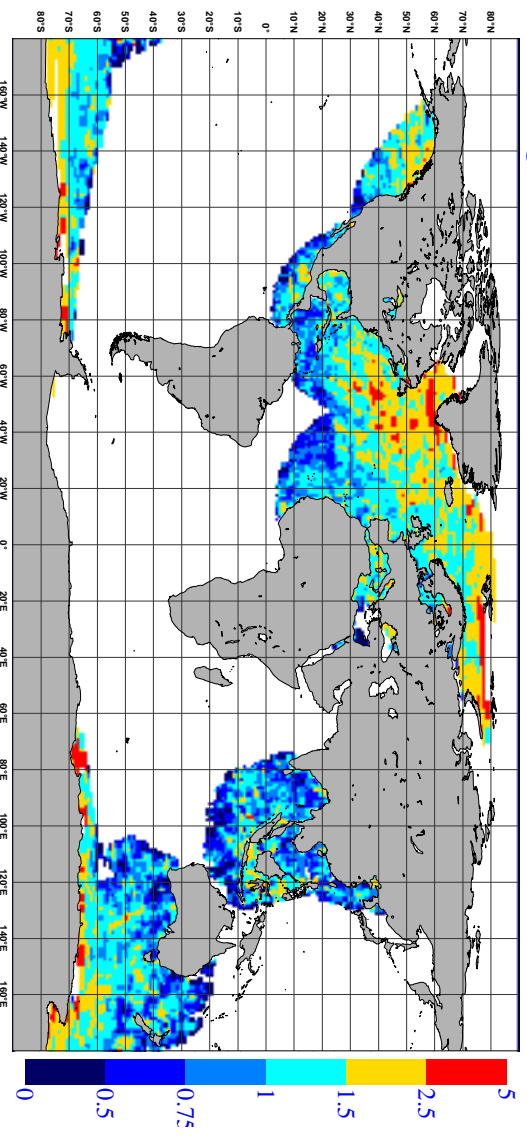


Figure 3

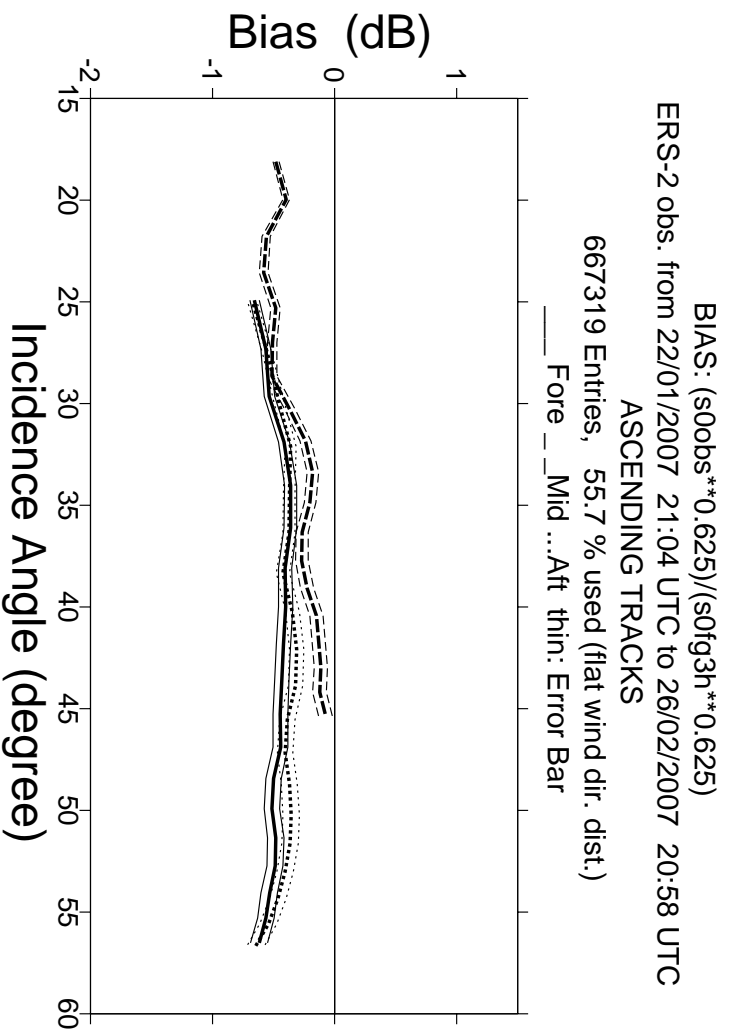
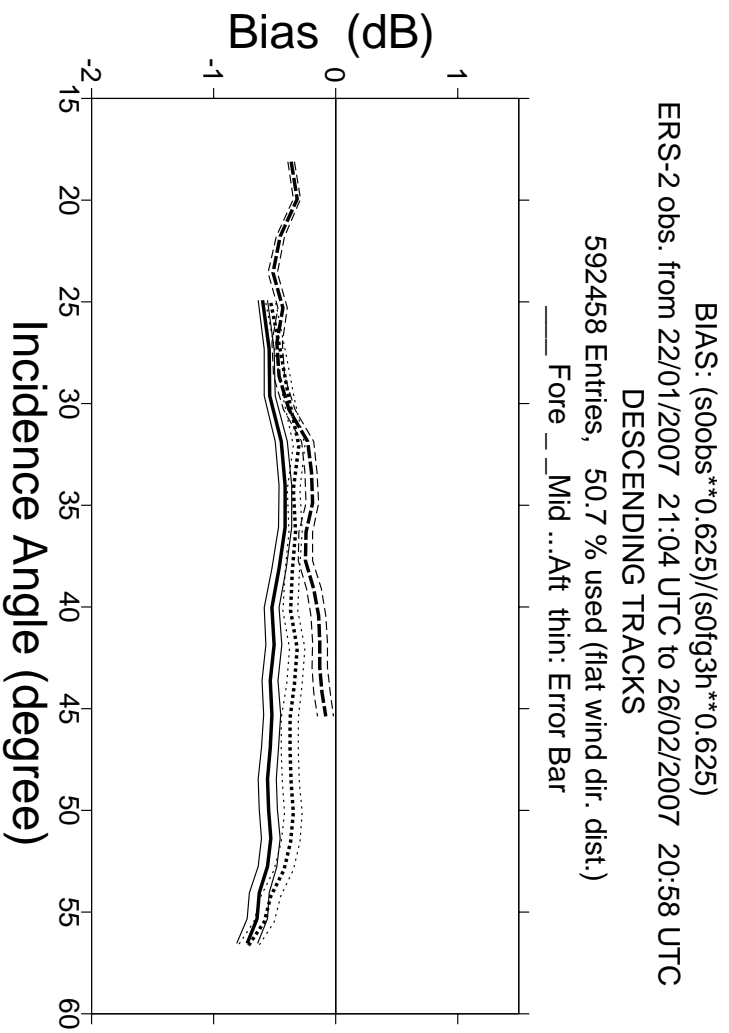


Figure 4

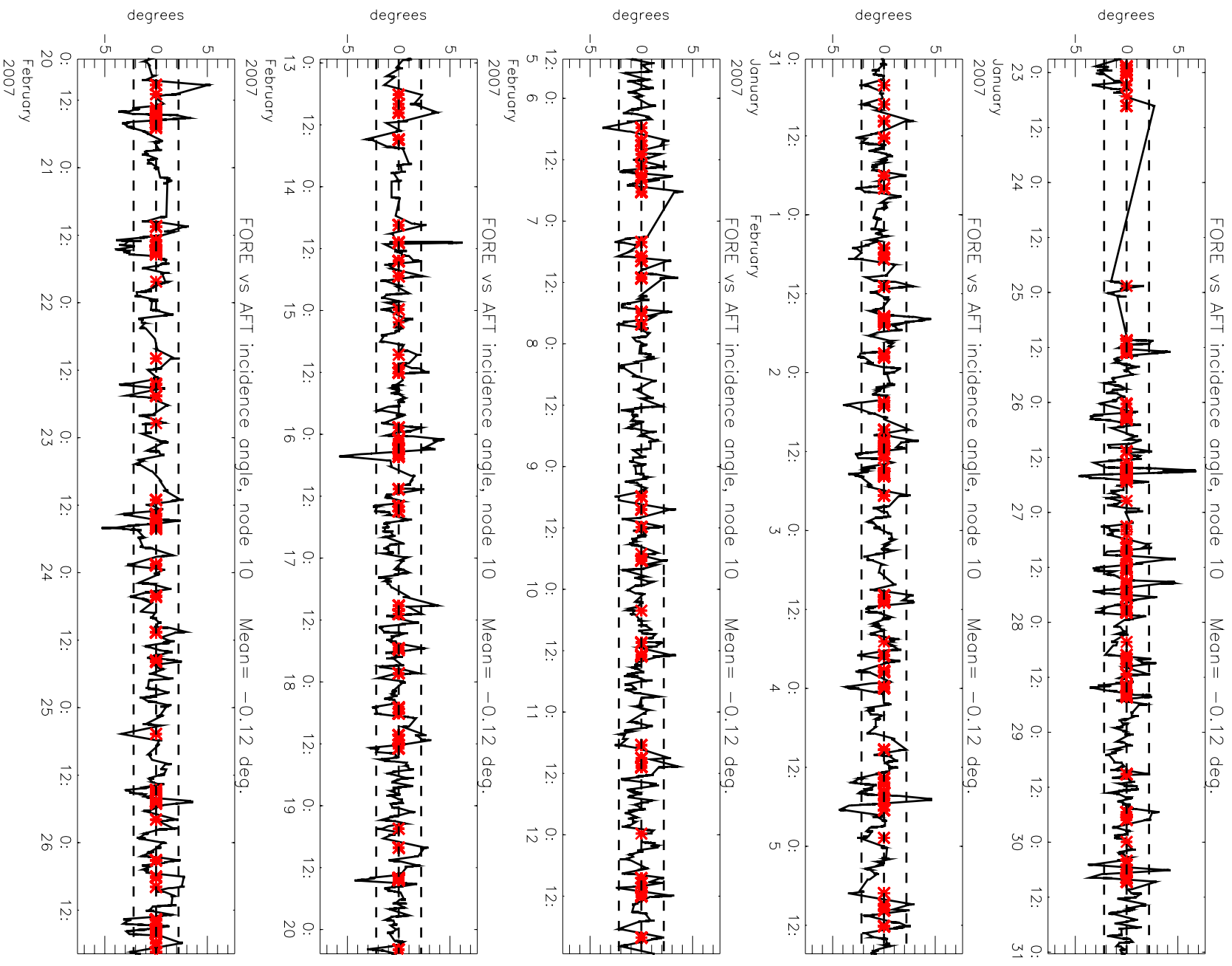


Figure 5

# Monitoring of Sigma0 triplets versus CMOD4 for ERS-2

from 2007012300 to 2007022618

(solid) mean normalised distance to the cone over 6 h

(dashed) fraction of complete sea-point observations rejected by ESA flag or CMOD4 inversion

(dotted) total number of data in log. scale (1 for 60000)

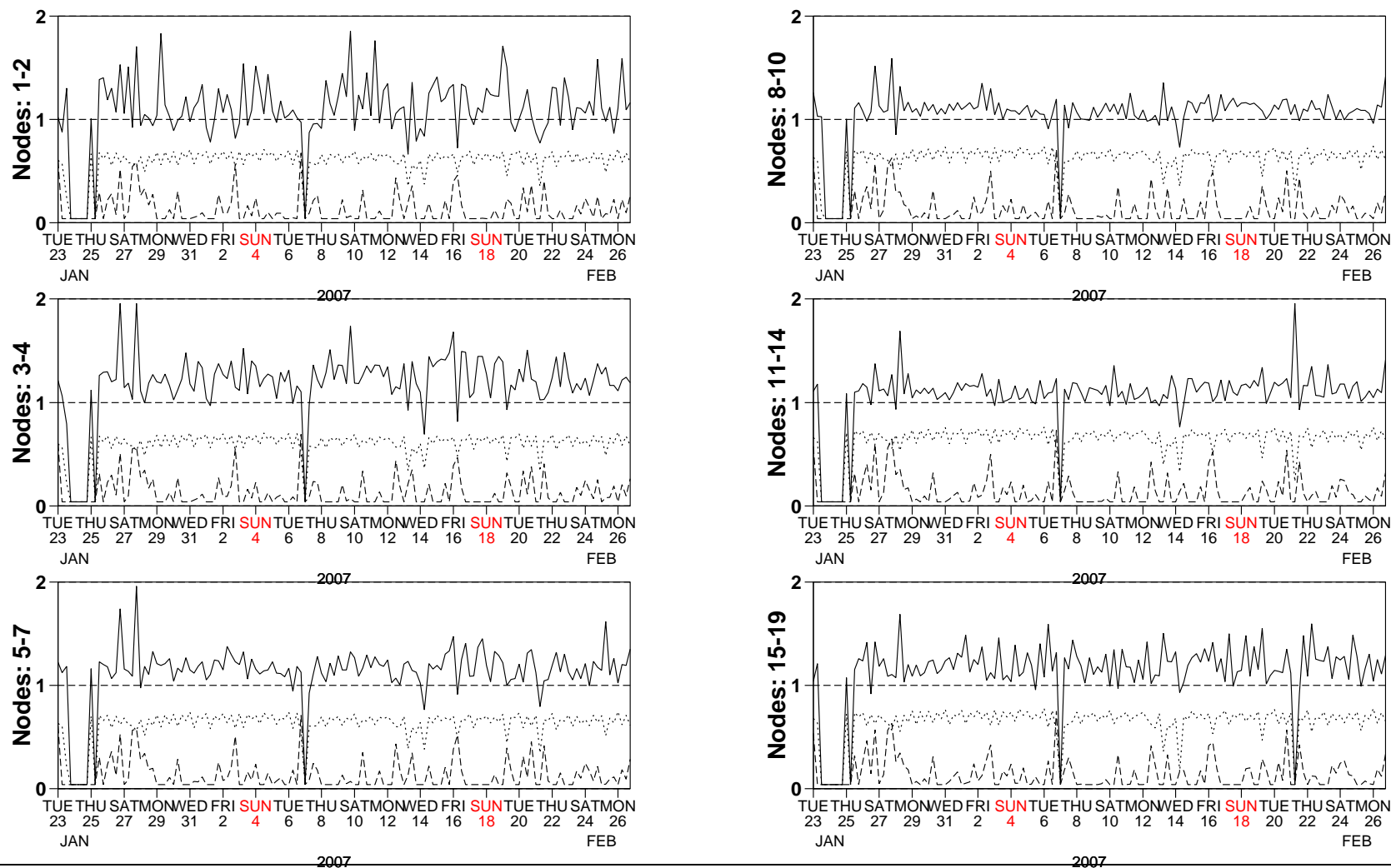


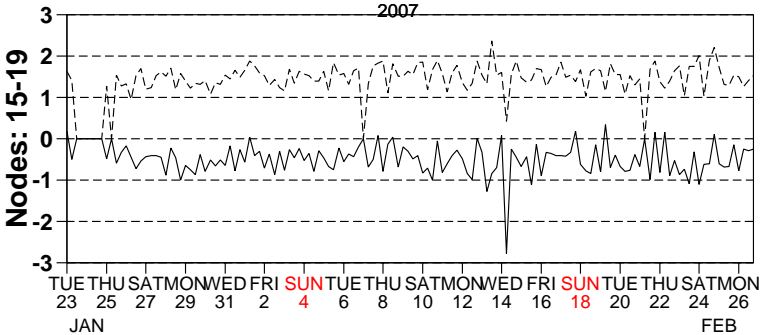
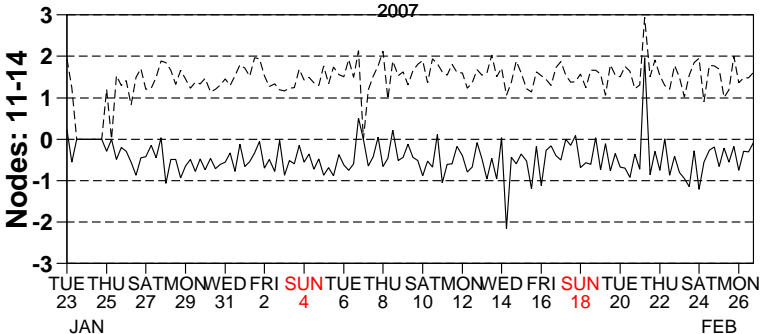
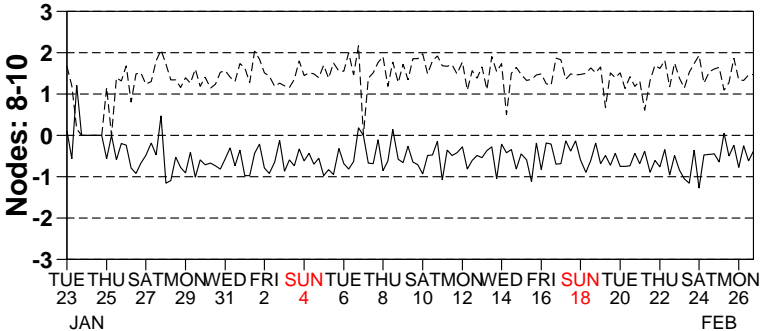
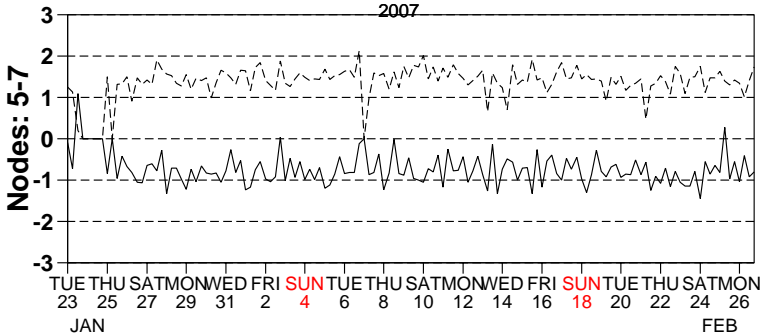
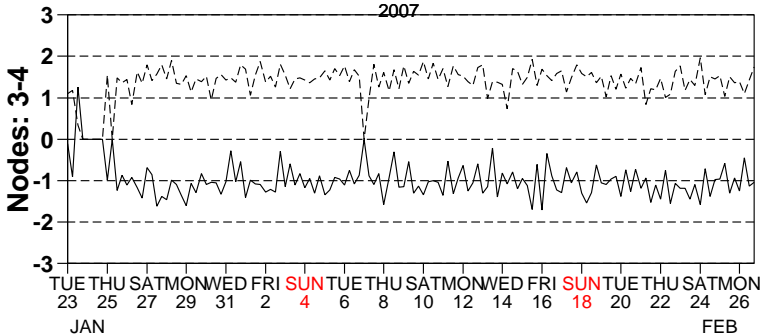
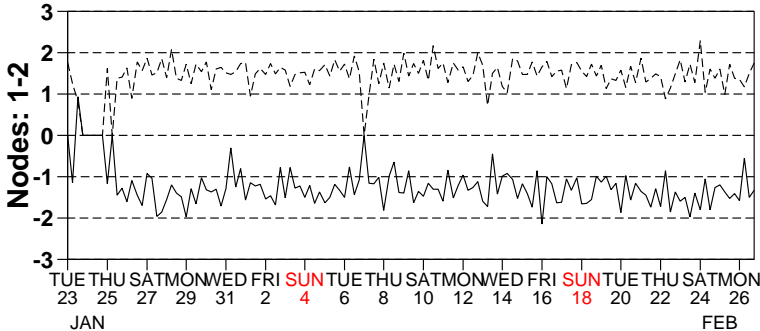
Figure 6

# Monitoring of UWI winds versus First Guess for ERS-2

from 2007012300 to 2007022618

(solid) wind speed bias UWI - First Guess over 6h (deg.)

(dashed) wind speed standard deviation UWI - First Guess over 6h (deg.)



2007

2007

Figure 7

# Monitoring of UWI winds versus First Guess for ERS-2

from 2007012300 to 2007022618

(solid) wind direction bias UWI - First Guess over 6h (deg.)

(dashed) wind direction standard deviation UWI - First Guess over 6h (deg.)

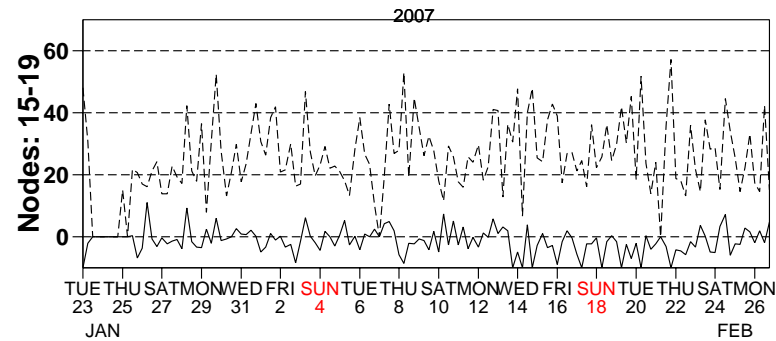
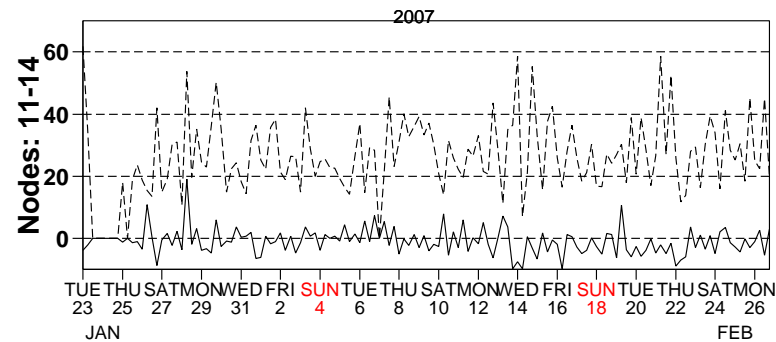
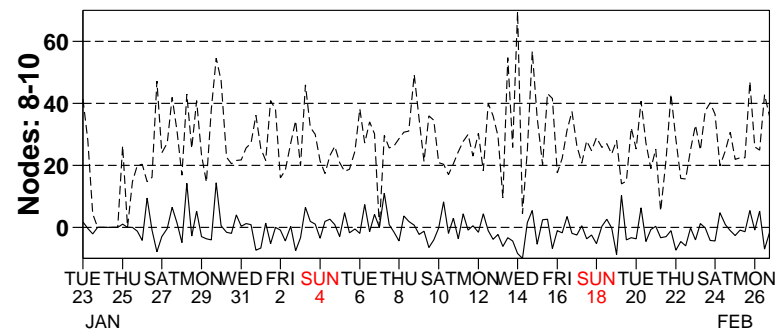
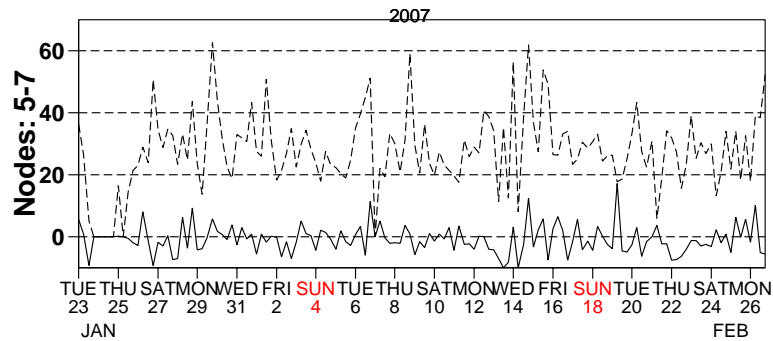
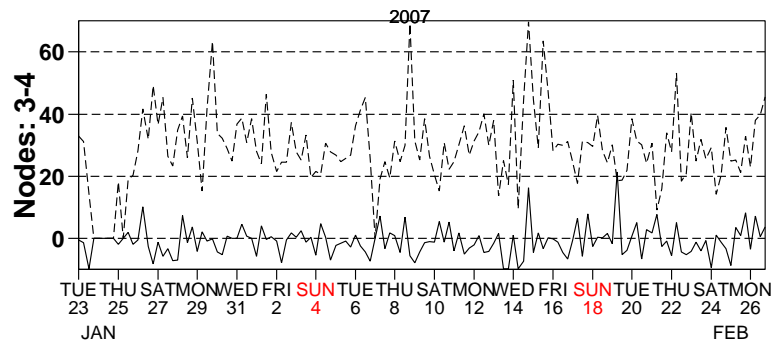
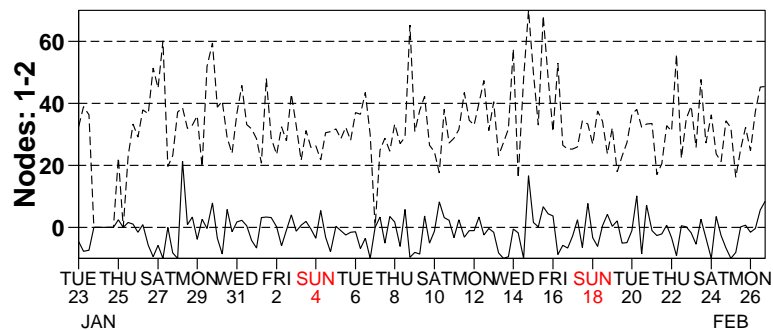


Figure 8

# Monitoring of de-aliased CMOD4 winds versus First Guess for ERS-2

from 2007012300 to 2007022618

(solid) wind speed bias CMOD4 - First Guess over 6h (deg.)

(dashed) wind speed standard deviation CMOD4 - First Guess over 6h (deg.)

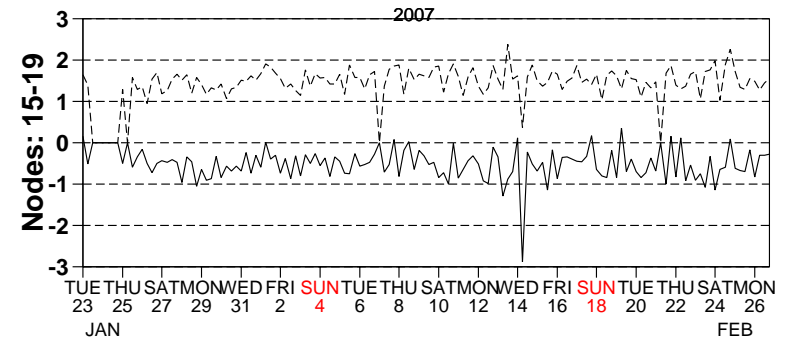
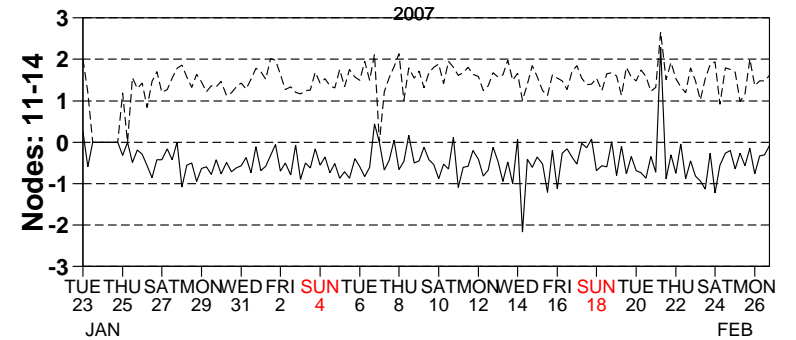
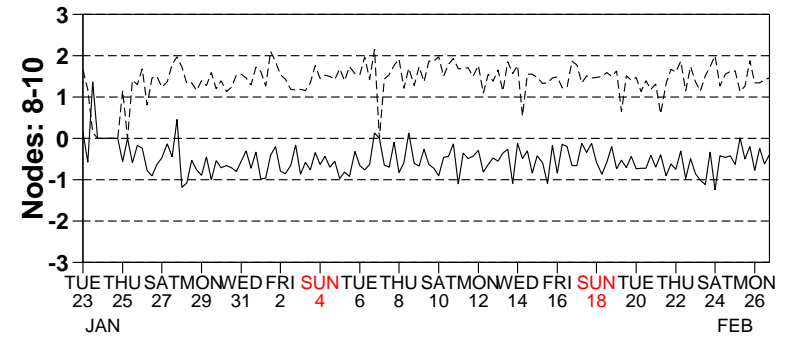
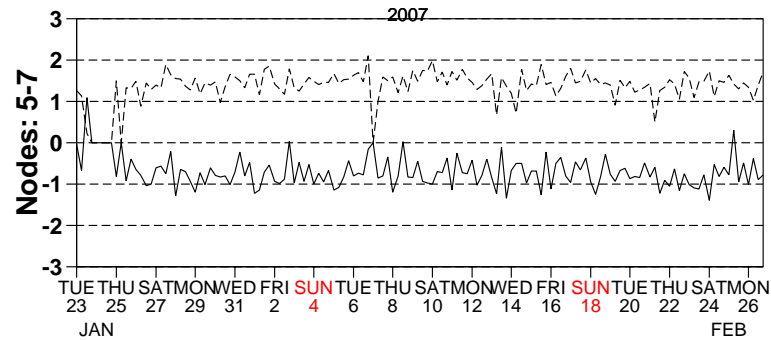
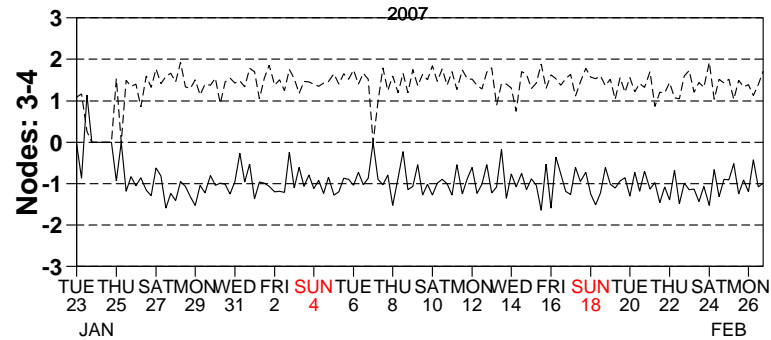
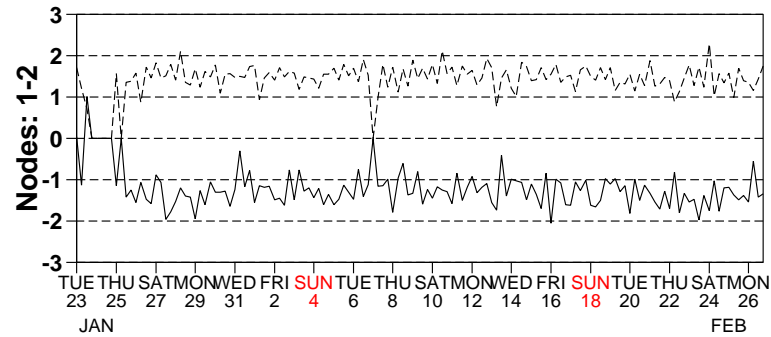


Figure 9

# Monitoring of de-aliased CMOD4 winds versus First Guess for ERS-2

from 2007012300 to 2007022618

(solid) wind direction bias CMOD4 - First Guess over 6h (deg.)

(dashed) wind direction standard deviation CMOD4 - First Guess over 6h (deg.)

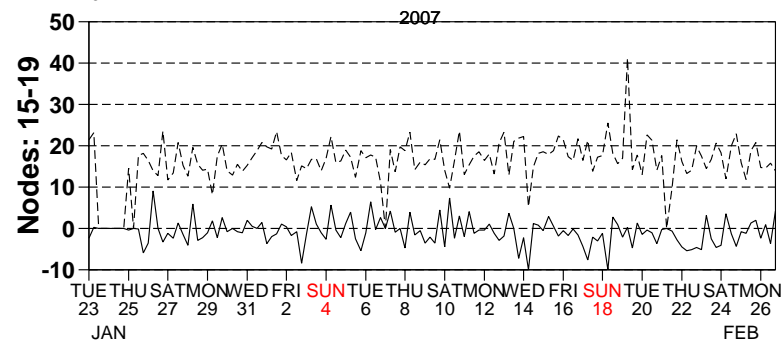
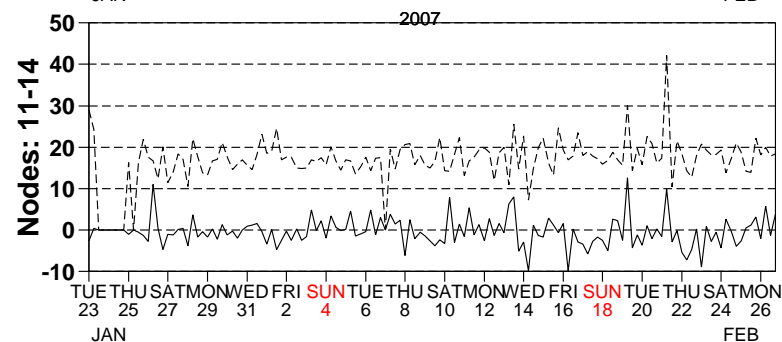
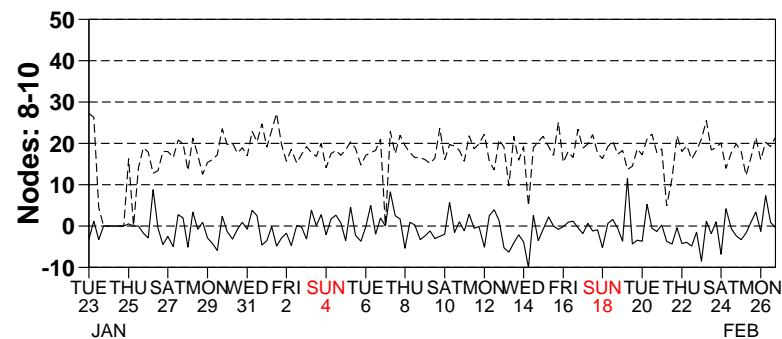
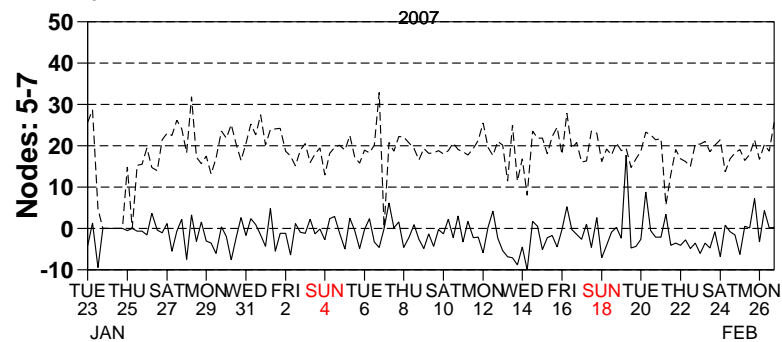
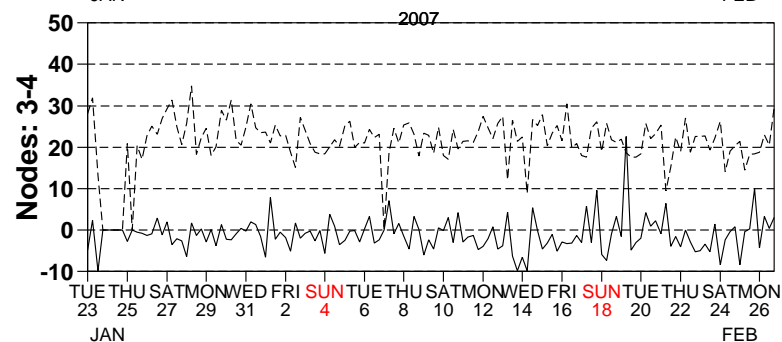
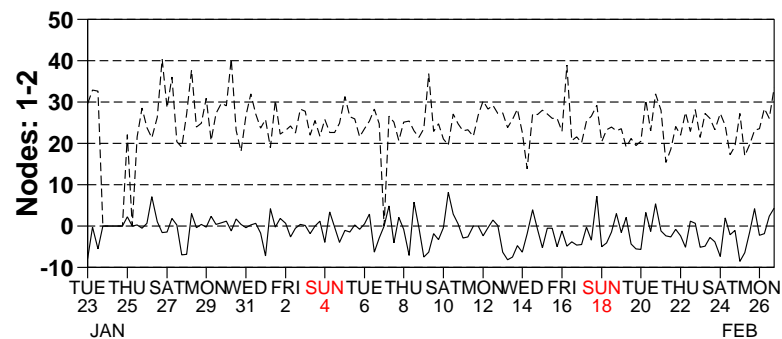
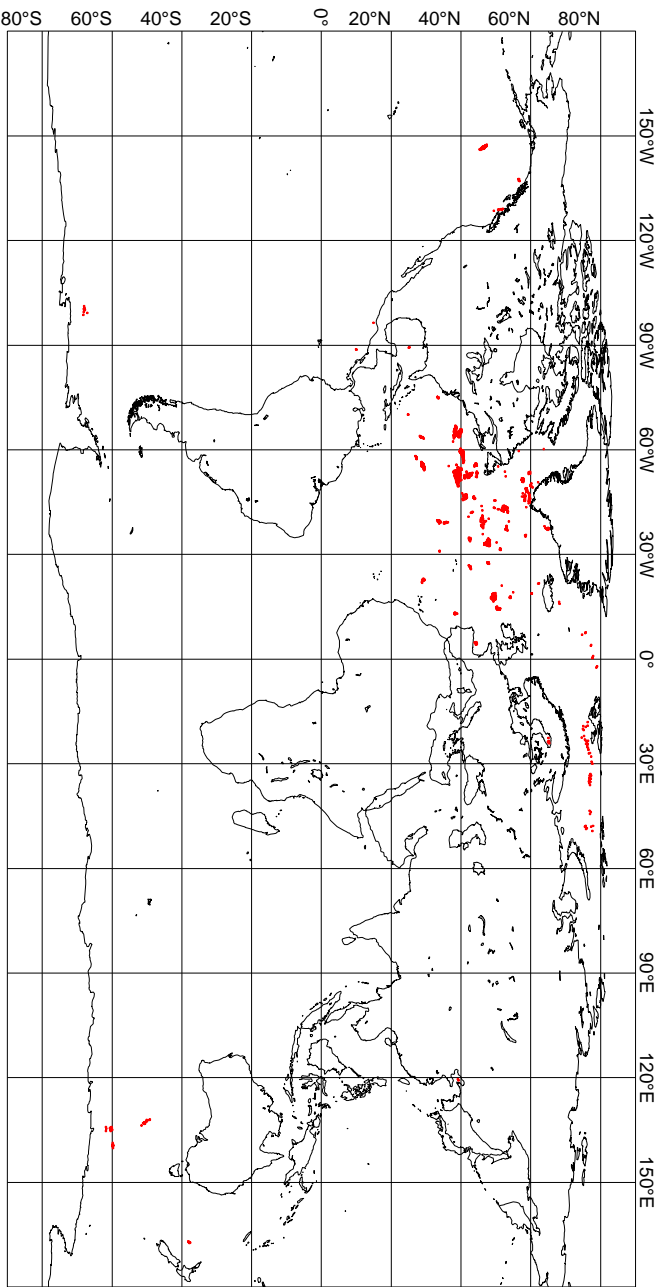


Figure 10



UWI winds more than 8 m/s weaker than ECMWF First Guess  
CYCLE 123, 2007012300 to 2007022618, QC on ESA flags



UWI winds more than 8 m/s stronger than ECMWF First Guess  
CYCLE 123, 2007012300 to 2007022618, QC on ESA flags

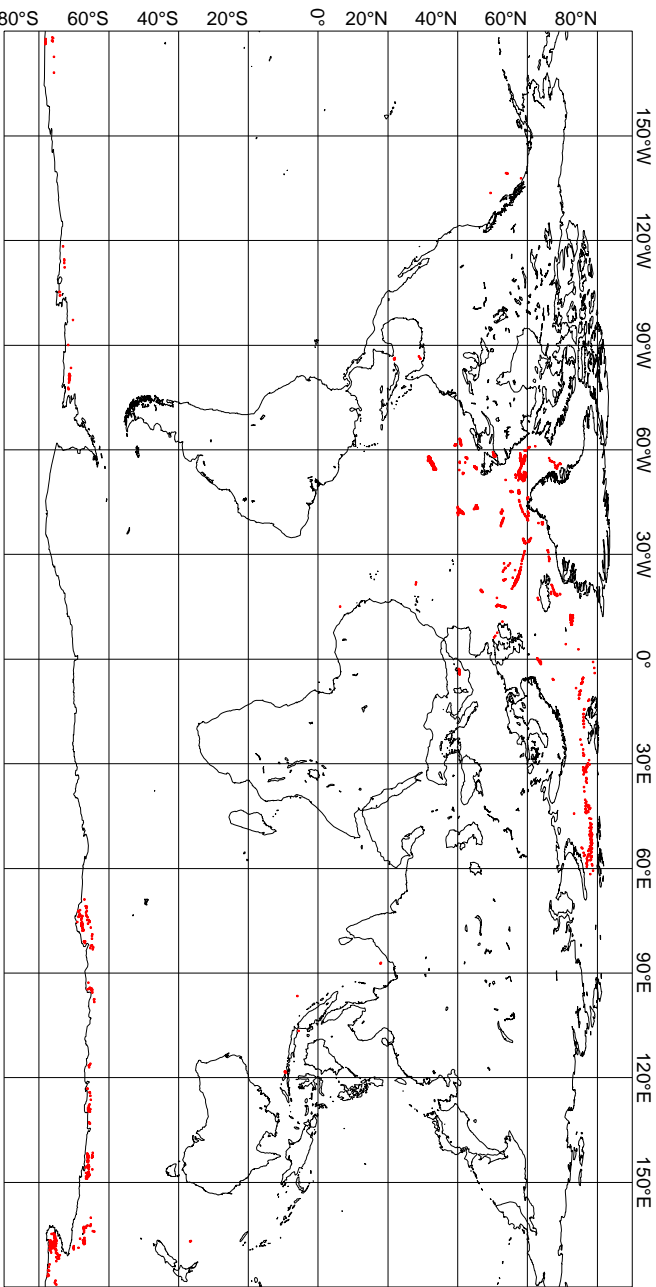


Figure 11

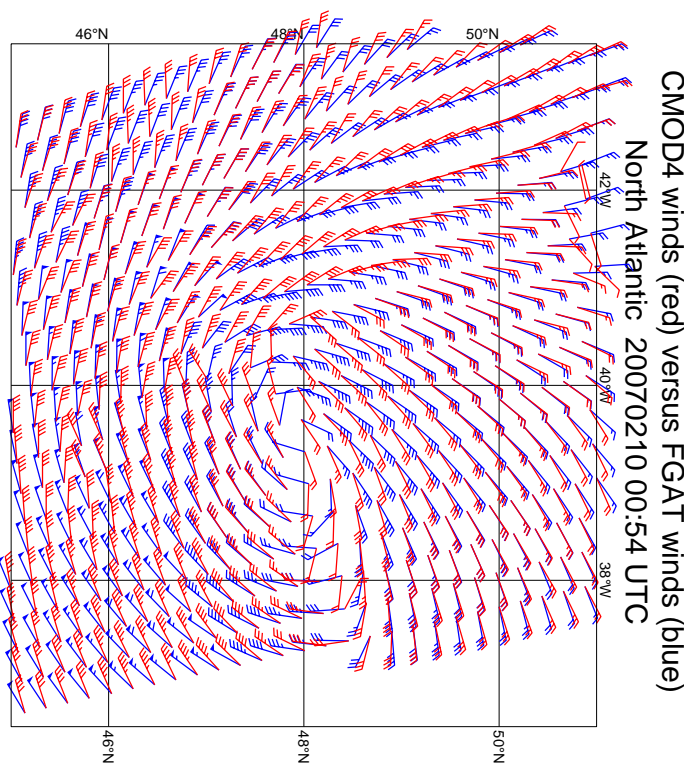
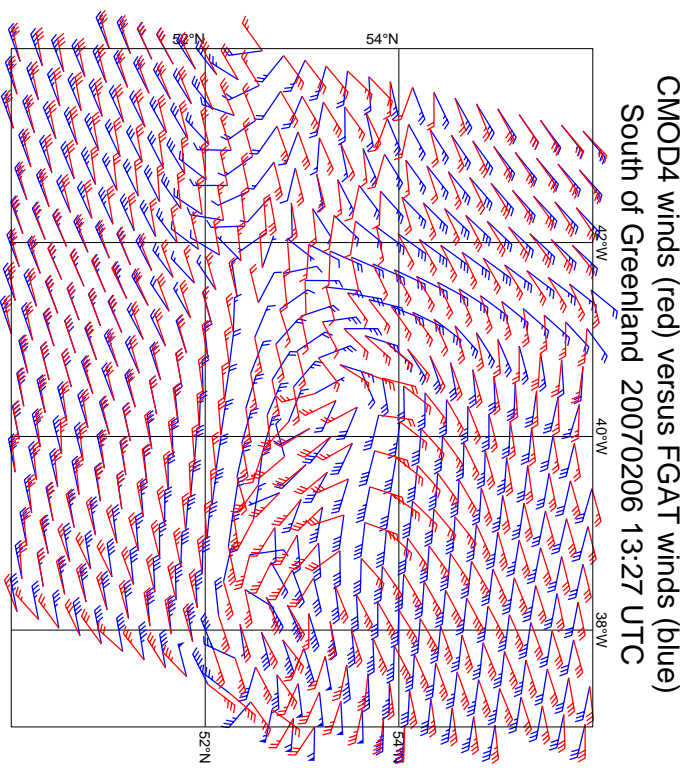


Figure 12

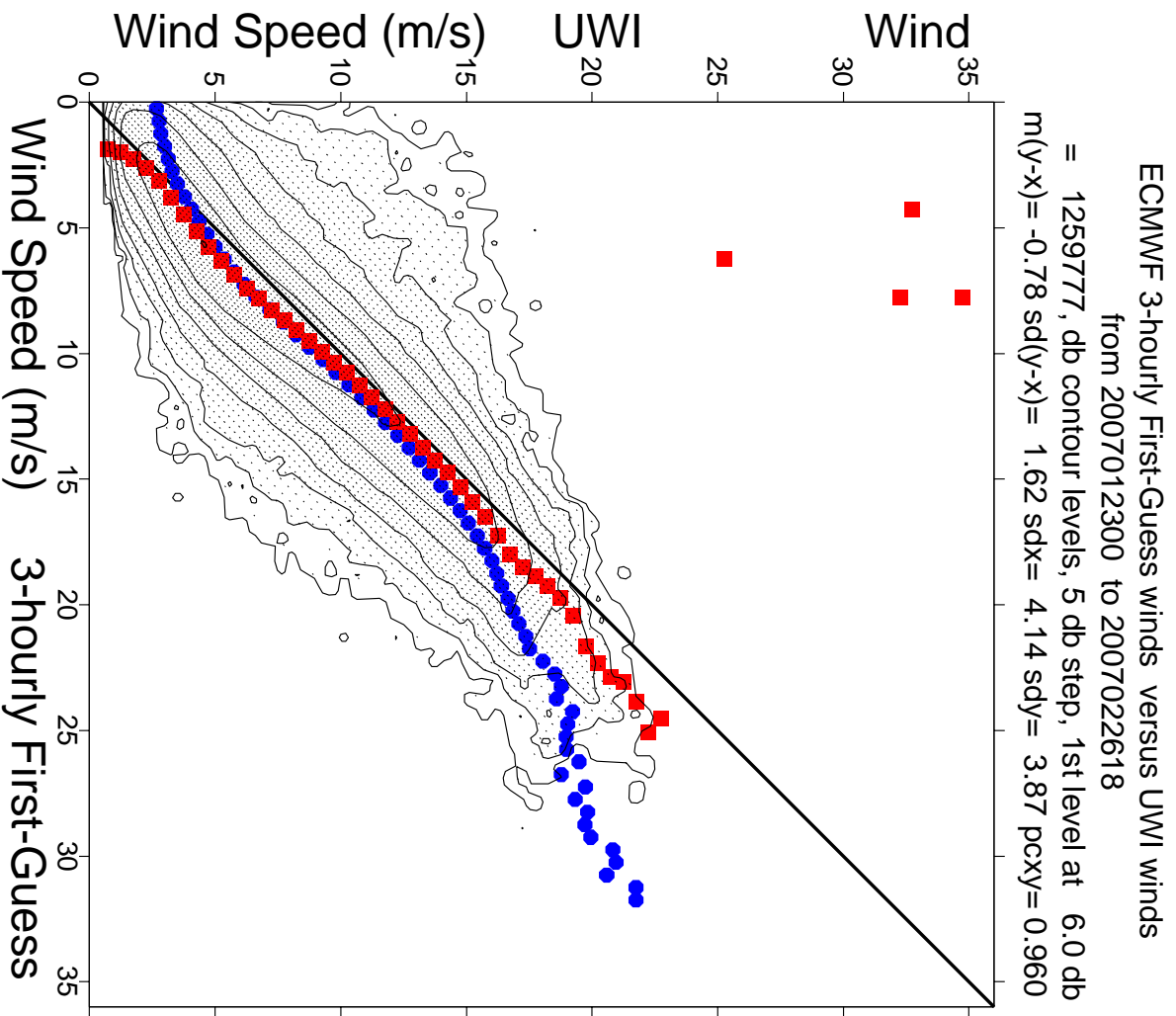


Figure 13

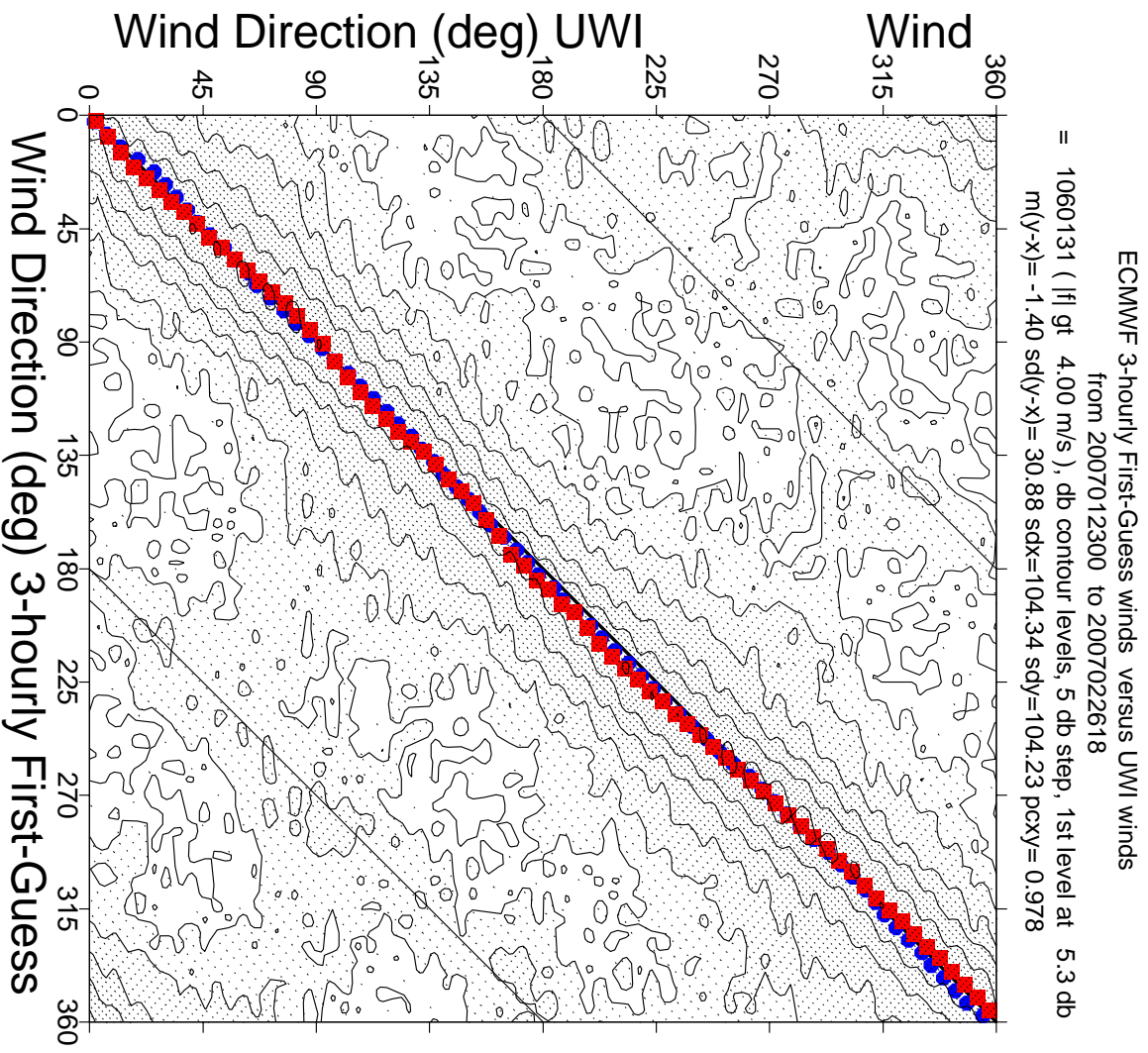


Figure 14

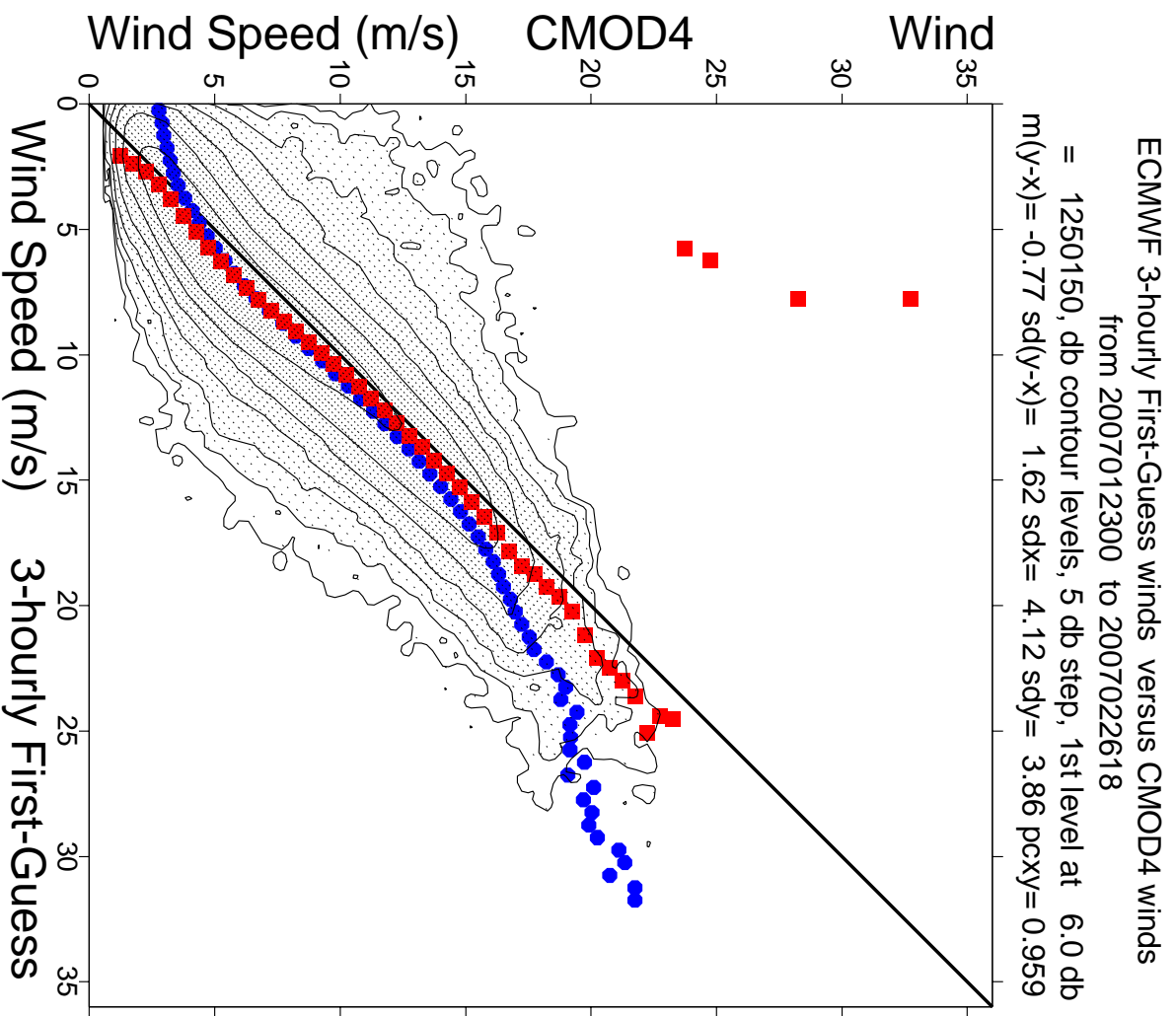


Figure 15

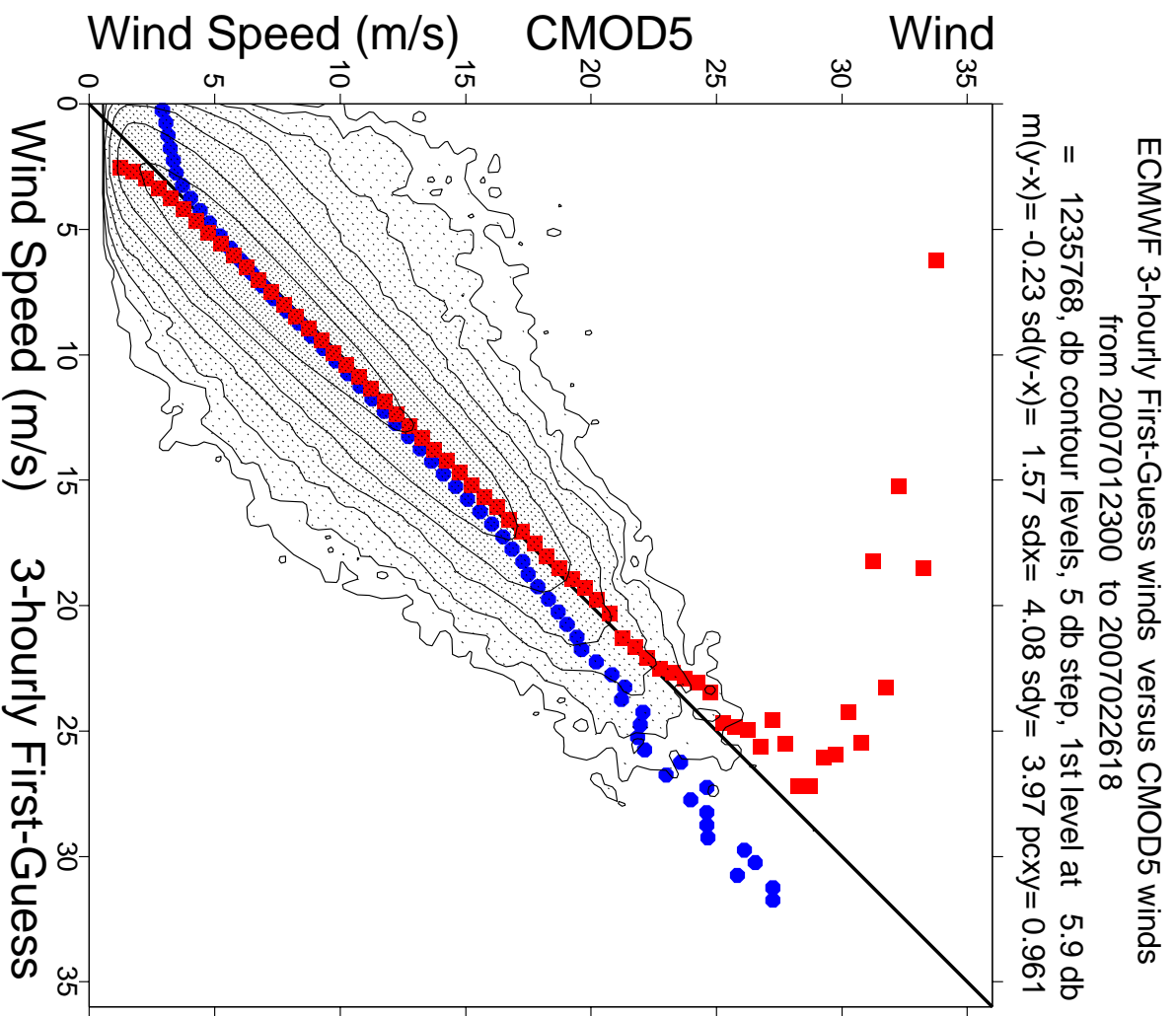


Figure 16

Figure 17

